Accurate modeling of InGaN quantum wells

Hans Wenzel
Ferdinand–Braun–Institut für Höchstfrequenztechnik
Gustav–Kirchhoff-Str. 4
12489 Berlin
Germany

***Abstract*— The internal field, the band structure and the oscillator strengths of the optical transitions of wurtzite strained InGaN QWs are accurately computed by a self–consistent solution of the Poisson equation and an eight–band $\boldsymbol{k}\cdot\boldsymbol{p}$ Schrödinger equation taking into account charges due to polarization fields, doping and free carriers. The results are used to investigate the dependence of the luminescence and gain spectra on the carrier injection.**

I. Introduction

Due to spontaneous and piezoelectric polarization fields, the computation of luminescence and gain spectra of wurtzite InGaN QWs necessitates the self–consistent solution of Poisson and Schrödinger equations for the determination of Hartree potential, energy bands and wave functions. Compared to previous work, the approach presented here is distinguished by the following features:

- The Poisson equation is solved in a larger domain than the Schrödinger equation. This allows a more accurate computation of the Hartree potential under the influence of macroscopic polarization fields, space charges and external bias because of a proper choice of the boundary values.
- The solution of the Schrödinger equation is based on $\boldsymbol{k}\cdot\boldsymbol{p}$ theory taking into account the three uppermost valence bands and the lowest conduction band, all doubly degenerated. One advantage of using an 8×8 Kane–like Hamiltonian with the appropriate wurtzite 6×6 part [1] describing the valence bands consists in the fact that the momentum operator needed for the calculation of the oscillator strengths can be simply calculated by the $\boldsymbol{k}$ gradient of the Hamiltonian. Moreover, the interband matrix elements get an additional term linear in $\boldsymbol{k}$, which is missed in six-band models with a separate treatment of the conduction band [2]. Another advantage is that the nonparabolicity of both the valence bands and the conduction band is accounted for, the latter is especially important for the small-band gap semiconductor InN.
- The quantum carrier densities are determined taking into account not only the fundamental electron and hole quantum states as done in previous approaches [3] but also higher order states. Similarly, not only single but also multi quantum wells can be handled.
- The carrier injection is parametrised in terms of the Fermi voltage and not in terms of an excess carrier density which can not be unambiguously defined.

II. Theory

The $\boldsymbol{k}\cdot\boldsymbol{p}$ Schrödinger equation to be solved reads

$$\mathbf{H}\big(e\phi_{\mathrm{H}}, V_{\mathrm{XC}}(n,p), \boldsymbol{k}_{||}, \frac{d}{dz}, z\big)\Psi_n(\boldsymbol{k}_{||}, z) = E_n(\boldsymbol{k}_{||}, z)\Psi_n(\boldsymbol{k}_{||}, z) \tag{1}$$

with the 8×8 Hamiltonian $\mathbf{H}$ taking into account the three uppermost valence bands and the lowest conduction band, all doubly degenerated, and the in–plane wave vector $\boldsymbol{k}_{||} = (k_x, k_y)$. Eq. (1) is solved subject to homogeneous Dirichlet conditions at the boundaries of the quantum region. The bulk conduction and valence band edges entering Eq. (1) are renormalized by Coulomb, exchange and correlation interactions according to

$$\begin{aligned} E_c^* &= E_c - e\phi_{\mathrm{H}} - \frac{1}{2}V_{\mathrm{XC}}\big(\frac{n+p}{2}\big) \\ E_v^* &= E_v - e\phi_{\mathrm{H}} + \frac{1}{2}V_{\mathrm{XC}}\big(\frac{n+p}{2}\big), \end{aligned} \tag{2}$$

where V_{XC} is the exchange–correlation potential in local density approximation and ϕ_{H} is the Hartree potential obtained from Maxwell's (Poisson) equation

$$\operatorname{div}\boldsymbol{D} = \rho - \operatorname{div}\boldsymbol{P} \quad \text{with} \quad \boldsymbol{D} = -\varepsilon_0\varepsilon_r \operatorname{grad}\phi_{\mathrm{H}} \tag{3}$$

where $\boldsymbol{P}$ is the macroscopic polarization. The charge density ρ is given by

$$\rho = e(p - n + N_{\mathrm{D}}^+ - N_{\mathrm{A}}^-) \tag{4}$$

with the electron and hole densities n and p, respectively, and the ionized donor and acceptor densities N_{D}^+ and N_{A}^-, respectively. Both the quantum (2D) carrier densities obtained from a summation over of all conduction and valence band states and the free (3D) carrier densities contribute to n and p. Eq. (3) is solved subject to the boundary conditions

$$\phi_{\mathrm{H}}(0) = 0 \quad \text{and} \quad \phi_{\mathrm{H}}(L) = \xi(L) - \xi(0), \tag{5}$$

where the electron chemical potentials ξ at $z = 0$ and $z = L$ are solutions of the bulk neutrality condition

$$N_v\mathrm{F}_{1/2}\Big(\frac{V_{\mathrm{F}} - E_{\mathrm{g}} - e\xi}{k_{\mathrm{B}}T}\Big) - N_c\mathrm{F}_{1/2}\Big(\frac{e\xi}{k_{\mathrm{B}}T}\Big) + N_{\mathrm{D}}^+ - N_{\mathrm{A}}^- = 0 \tag{6}$$

with the difference of the electro–chemical potentials (Fermivoltage) $V_{\mathrm{F}} = e\phi_n - e\phi_p$ acting as an input parameter (compare Fig. (1)). In Eq. (6), parabolic bands are assumed and the splitting of the valence band into three bands at $\boldsymbol{k} = 0$ is neglected. N_c and N_v are the band edge density of states,

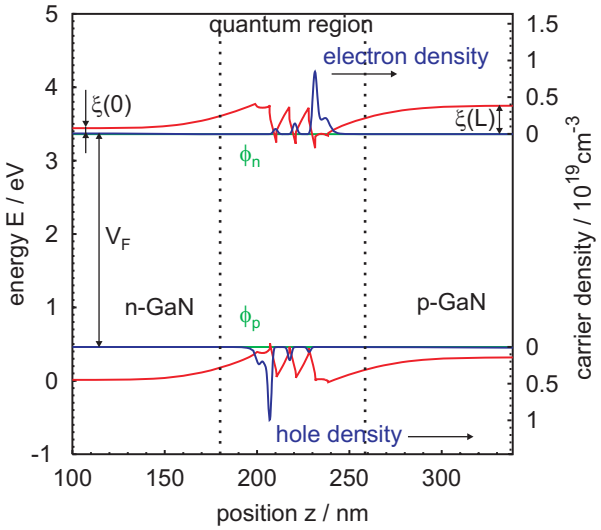

Fig. 1. Profiles of bulk band edges, electro–chemical potentials and carrier densities at $V_F = 2.9$ eV

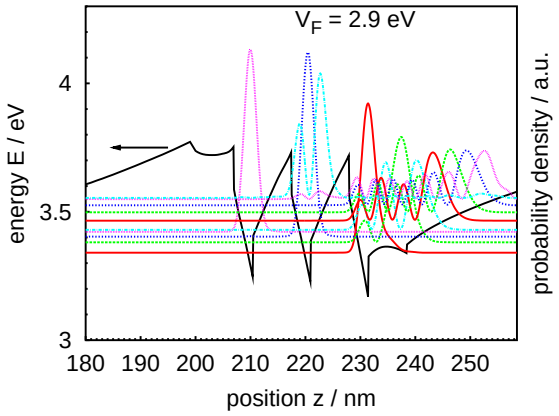

Fig. 2. Profiles of bulk conduction band edge and electron quantum probability densities at $V_F = 2.9$ eV

E_g is the energy gap and $F_{1/2}$ is a Fermiintegral. By fixing the energy origin, Eq. (6) pins the electro–chemical potentials which are assumed to be continuous and constant throughout the simulation domain.

Eqs. (1) and (3) are iteratively solved. In order to increase the stability and to speed up the convergence an implicit iteration scheme is used.

III. Results

In what follows an unintentionally doped ($N_D = 10^{16}$ cm^{-3}) InGaN triple quantum well (TQW) consisting of 3.5 nm thick $In_{0.09}Ga_{0.91}N$ wells and 7 nm thick $In_{0.015}Ga_{0.985}N$ barriers embedded in n– and p–doped GaN layers ($N_D = 10^{17}$ cm^{-3} and $N_A = 10^{17}$ cm^{-3}, respectively) is considered.

Fig. 1 shows the calculated bulk band edges, electro-chemical potentials and carrier density profiles for a Fermi voltage of $V_F = 2.9$ eV which is well below the value for laser threshold, appropriate for luminescence investigations.

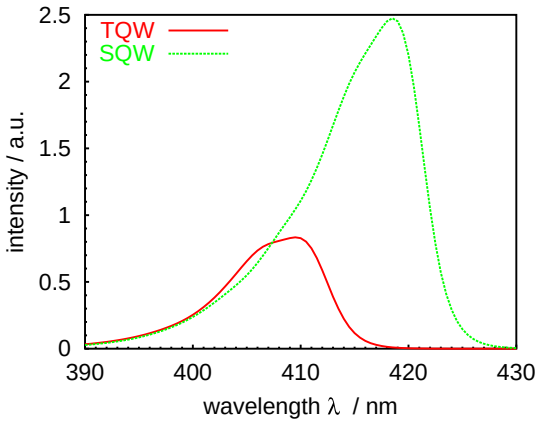

Fig. 3. Luminescence spectra for TQW and SQW at $V_F = 2.9$ eV

Due to the internal electric field caused by the polarization charges, only the outer wells are substantially populated with a spatial separation of the maxima of the electron and hole densities.

The corresponding electron quantum probability densities together with the bulk conduction band edge are shown in Fig. 2. The potential of the first well and of the second well is almost triangular shaped so that the maximum of the probability densities of the fundamental electron states of these wells are located at the interface between the wells and the corresponding right barriers. However, the third well forms together with the last InGaN barrier and part of the p-GaN layer a “new” thicker well, where several electron states are located. A similar picture holds for the holes.

The strong spatial separation of the electron and hole probability densities decreases the oscillator strengths of the optical transitions, which leads to a reduction of the luminescence intensity. This is depicted in Fig. 3, where the luminescence spectrum of the TQW structure is compared with that of a corresponding single quantum well (SQW). A sech-type of broadening was employed with $\Delta E = 10$ meV. Besides a reduction of the intensity also a blue–shift of the peak wavelength can be observed.

Due to the fact, that luminescence spectra can be easily measured, they are sometimes used to fit parameters entering theoretical models for the computation of gain spectra [4]. The main conclusion here is, that for InGaN QWs it is not sufficient to consider only a single quantum well as it is mostly done, but one has to consider the whole optical active structure. At the conference, further details of the computational approach and results including gain spectra will be presented. We will also investigate different approaches to realize a more uniform carrier distribution in the MQW structure, e.g. by doping the barriers.

References

[1] S. L. Chuang *et al.*, Phys. Rev. B, vol. 54, pp. 2491-2504 (1996)
[2] P. Enders *et al.*, Phys. Rev. B, vol. 51, pp. 16695-16704 (1995)
[3] W. Chow *et al.*, Phys. Rev. B, vol. 60, pp. 1947-1952 (1999)
[4] J. Hader *et al.*, IEEE Photon. Techn. Lett., vol. 14, pp. 762-764 (2002)